



CHALMERS

Chalmers Publication Library

Study of Q-Factors of Ridge and Groove Gap Waveguide Resonators

This document has been downloaded from Chalmers Publication Library (CPL). It is the author's version of a work that was accepted for publication in:

IET Microwaves, Antennas & Propagation (ISSN: 1751-8725)

Citation for the published paper:

Pucci, E. ; Zaman, A. ; Rajo-Iglesias, E. (2013) "Study of Q-Factors of Ridge and Groove Gap Waveguide Resonators". IET Microwaves, Antennas & Propagation, vol. 7(11), pp. 900-908.

<http://dx.doi.org/10.1049/iet-map.2013.0081>

Downloaded from: <http://publications.lib.chalmers.se/publication/182464>

Notice: Changes introduced as a result of publishing processes such as copy-editing and formatting may not be reflected in this document. For a definitive version of this work, please refer to the published source. Please note that access to the published version might require a subscription.

Chalmers Publication Library (CPL) offers the possibility of retrieving research publications produced at Chalmers University of Technology. It covers all types of publications: articles, dissertations, licentiate theses, masters theses, conference papers, reports etc. Since 2006 it is the official tool for Chalmers official publication statistics. To ensure that Chalmers research results are disseminated as widely as possible, an Open Access Policy has been adopted. The CPL service is administrated and maintained by Chalmers Library.

(article starts on next page)

Study of Q-Factors of Ridge and Groove Gap Waveguide Resonators

Elena Pucci¹, Ashraf Uz Zaman¹, Eva Rajo-Iglesias^{1,2}, *Senior Member, IEEE*, Per-Simon Kildal¹, *Fellow, IEEE*
and Ahmed Kishk³, *Fellow, IEEE*

¹Department of Signals and Systems, Chalmers University of Technology, SE-41296 Gothenburg, Sweden

e-mail: elena.pucci@chalmers.se; zaman@chalmers.se; per-simon.kildal@chalmers.se

²Department of Signal Theory and Communication, University Carlos III of Madrid, Avda Universidad 30,

28911 Leganes (Madrid), Spain

e-mail: eva@tsc.uc3m.es

³Department of Electrical and Computer Engineering, Concordia University, Montreal, Quebec, Canada

e-mail: kishk@ece.concordia.ca

Abstract

The gap waveguide technology for millimeter waves applications has been recently presented. The new structure is made by generating a parallel plate cut-off region between an artificial magnetic conductor (AMC) and a metallic plate. Propagating waves will be only allowed to follow a metal ridge or groove surrounded by the AMC. The gap waveguide can be made of only metal and does not need any contact between the metal joints compared to standard waveguides. In this paper, a study of Q-factors of resonators made in ridge and groove gap waveguides are presented. The resonators are made of copper and the AMC used is a textured surface of metallic pins. Simulated and measured unloaded Qs are presented and compared with Q of a standard rectangular waveguide. High Q-factors are measured for the prototypes presented, approaching 90-96% of the simulated values. Furthermore, it is shown how the

lid of pins can easily stop the leakage loss at the joints of the circuit, which is the typical cause of reduced Q-factor of standard waveguides at high frequency.

***Index Terms*—Artificial magnetic conductors, gap waveguide technology, losses, quality factor, waveguides resonators.**

I. INTRODUCTION

The development of wireless and satellite communication systems has led to a demand of high performance microwave and mm-wave components in terms of costs, lower loss, compact size and compatibility with other RF circuit elements to be included in a complete antenna system. Rectangular waveguide technology is traditionally used because of its low loss, i.e. high Q-factor, but the fabrication becomes complex and expensive at high frequencies. Also, rectangular waveguides can be difficult to integrate in one unique electronic module containing active components and MMICs (monolithic microwave integrated circuits) mounted on printed circuits boards and interconnected with microstrip circuits. On the other hand, planar transmission lines, such as microstrip and stripline, are in comparison lossy due to the use of dielectric materials, and they suffer from unwanted radiation losses or associated problems related to packaging and shielding.

During the last couple of years, a new transmission line technology, called *gap waveguide*, has been presented [1]-[3]. The gap waveguide is ideally made of two parallel plates, the upper one a perfect electric conductor (PEC) and the lower one a perfect magnetic conductor (PMC). When the distance between these parallel plates is smaller than quarter wavelength, a parallel plate cut-off region will be generated in the gap between the PEC and the PMC plates. Waveguides appear within this gap when PEC strips or ridges are formed within or above the PMC surface. The wave will propagate between the PEC strip (or ridge) and the PEC plate, bounded on both sides by the cut-off between the PEC and PMC surfaces. The PMC condition can be realized by making use of high impedance surfaces, such as the “bed of nails” [4], which is a periodic surface made of metallic pins readily manufactured by milling and suitable for high frequency applications. Also, other textured surfaces generating high surface impedance can be used, often referred to as artificial magnetic conductors (AMC) or electromagnetic bandgap (EBG) surfaces due to the non-existence of surface waves within a bandgap. An example of AMC is the mushroom-type surface [5], which is more compact than nails at lower frequencies. A numerical study in terms of parallel plate stop-band generated by different AMCs for gap waveguide is presented in [6] where it is shown that stop bands up to 4:1 can be achieved.

In the realized gap waveguide the direction of the propagating wave is controlled and only allowed to follow a desired path, along a metal strip, ridge or groove, surrounded by the AMC surface [1]. For this reason, the *ridge gap waveguide* refers to a new type of transmission line where the quasi-TEM mode is propagating in the gap between a ridge and an upper metal plate, and outside

this region all local parallel plate modes are stopped by the AMC surface. It should be mentioned that the gap waveguide is naturally shielded and has no radiation losses. Experimental validation for this solution has already been presented in [7].

This new gap waveguide approach is based on the known concept of soft and hard surfaces [8], and it is a consequence of the previous research on hard waveguides [9], [10] and ‘single-hard-wall’ waveguides [11]. The latter describes for the first time local gap waves propagating along ridges between corrugations. However, the geometries in [8]-[10] are very narrowband and often lossy compared to the gap waveguide.

The *groove gap waveguide* is a second version of gap waveguide technology [2], [12]. The configuration is the same as the ridge gap waveguide but in this case the ridge is replaced by a groove between the pins so that the structure behaves similar to a standard waveguide with propagating TE/TM modes. Substrate integrated waveguides (SIW) [13]-[14], are already used as alternatives to standard waveguides, but yet the substrate is needed. The SIW can be made thinner than gap waveguides, but then the conductive loss becomes significant [15]. Therefore, gap waveguides are advantageous compared to SIW, in particular at high frequency.

Ridge and groove gap waveguides are attractive alternatives to waveguides and conventional transmission lines, as they are made of only metal and easy to manufacture. They can also be used to package components [16]. The basic theories have already been developed in [17] where analytical solutions and dispersion characteristics are described, and in [18] where Green’s functions for the gap waveguide geometry are constructed in the plane wave spectral domain. In [19-21] it is shown how this new technology can be used to realize standard microwave components. In particular in [20], [21], pass band filters in groove gap waveguide are presented showing very good performance in terms of low insertion loss and high selectivity to avoid spurious close to the passband. The benefits of this technology are also shown in the independent research in [22].

One important step to go further on the validation of this new technology is the detailed study of losses. This is more crucial at millimeter and sub-millimeter waves where the manufacturing is more difficult, and losses are the factor affecting the most the circuit performance. In [23] we show a preliminary numerical study of losses for the ridge gap waveguide and compared with rectangular waveguides and microstrip lines. In the present paper we extend the study by including also the groove gap waveguide version, and experimental validations for both ridge and groove types, all realized by bed of nails, and compared with losses of normal rectangular waveguides. In addition, we study the attenuation at the joint between a shorting metal wall and the upper lid.

In order to verify the performance of the low loss gap waveguide technology, it is important to be able to characterize its loss in an accurate way. One way to do that is to measure the attenuation of a very long line, but it will be impractically long in order to measure the low losses accurately. As an alternative, losses can be better characterized in terms of Q factors of resonators.

Therefore, the studies of the present paper are performed by numerical and experimental investigation of Q-factors of gap waveguide resonators. The Q-factor approach is well established and known to give accurate results for transmission lines with low losses [24, Sec.6]. Even more, when dealing with TEM mode type of transmission line resonators, the attenuation can be easily extracted from the Q-factor as

$$\alpha = \frac{\beta}{2Q_U}, \quad (1)$$

where β is the propagation constant.

II. QUALITY FACTOR & LOSSES

The quality factor Q is the key characteristic parameter for many microwave circuits. It defines how much energy is dissipated in a system relative to the stored energy. Basically, it quantifies the loss in a resonant circuit [24, Sec.6]. The loaded Q (Q_L) can be expressed as

$$\frac{1}{Q_L} = \frac{1}{Q_U} + \frac{1}{Q_E}, \quad (2)$$

where Q_U is the unloaded quality factor, related to the loss of the circuit itself, and Q_E is the external quality factor due to the loss added by the loading resistor, which could represent the coupling circuit as well as the feeding network, and it is given by [25]

$$Q_E = 10^{\frac{[S_{21}(dB)]}{20}} \cdot Q_L, \quad (3)$$

for a two-port resonator, where S_{21} is the transmission coefficient of the resonator (ratio of the voltage transmitted to the incident voltage). Therefore, the unloaded Q-factor can be de-embedded [26] and obtained as follows

$$Q_U = \frac{Q_L}{1 - S_{21}}. \quad (4)$$

Note that this formula is only valid if there is no ohmic loss related to the coupling coefficient of the coaxial connectors at each end of the resonator. Thus, it will e.g. not be valid if we locate an attenuator at each port and measure the S-parameters through

the resonator including the attenuators. When the feeding circuit is weakly coupled to the resonator, the transmission coefficient S_{21} becomes very small so that the sensitivity of the measurements does not affect the amplitude of S_{21} . In this case Q_U is approximately equal to Q_L , as shown in (4), and it can be directly extracted by the following

$$Q_L = \frac{f_o}{\Delta f_{3dB}}, \quad (5)$$

where Q_L is defined as the ratio between the center frequency of the resonant cavity and its 3-dB bandwidth [24, Sec.6].

All the practical resonators measured in this paper are fed by SMA connectors, for convenience. The weak coupling is in this case achieved by cutting the inner conductor of the connectors to create a certain mismatch.

The simulated Q-factors are achieved first with HFSS eigenmode solver, which directly calculates the unloaded Q from the eigenmodes of the structure. However, the eigenmode solutions have some restrictions, e.g., they do not include losses due to the ports. Therefore, we simulated also the S_{21} of the resonators including SMA connectors and calculated the Q using equations (4)-(5). This last approach is the same used for the measurement. The unloaded Qs obtained from the eigenmode solver and from the simulated S_{21} are presented in Table I for each structure considered in this paper. Their discrepancy is a measure of uncertainty.

III. RIDGE GAP WAVEGUIDE RESONATOR

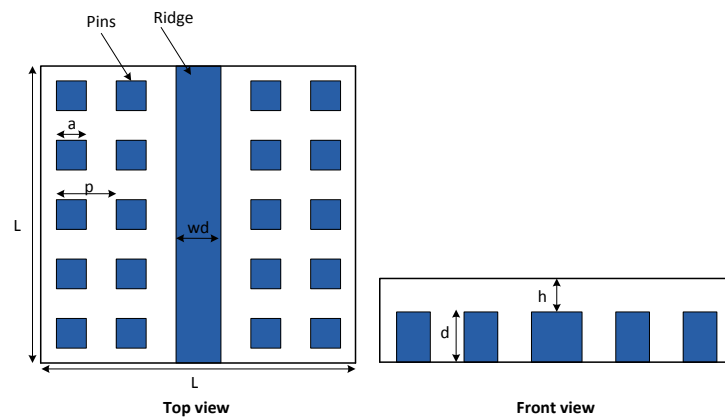
This section will show simulated and measured results for one short circuit and one open circuit transmission line resonator made in ridge gap waveguide.

A. Short Circuit Resonator

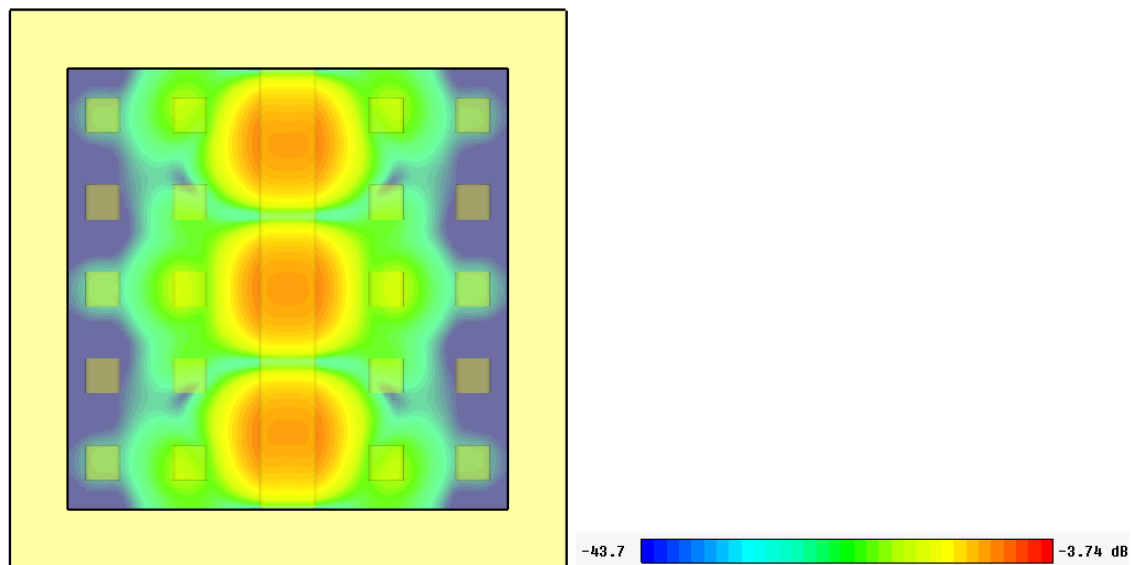
In this first design the ridge is surrounded by conducting pins on both sides whereas it is short circuited by metal walls at both ends, as shown in Fig. 1(a). The period of the pins is $p = 7.5$ mm, pin width is $a = 3$ mm, and resonant length $L = 38$ mm (i.e. 1.5 wavelengths) in order to obtain a third order resonance at around 13 GHz. The pins and ridge edges are rounded (the pins on two sides only) to decrease the loss due to sharp edges, as it was also presented in [23]. The height of pins and ridge is $d = 5$ mm and the width of the ridge is $wd = 5$ mm. As seen in [23], the loss decreases as the air gap h between the ridge and the upper lid increases. In this case, h is set to be 3 mm, corresponding to a characteristic impedance of about 148 Ω , using the approximate stripline formula in [7], and a parallel-plate stop band between 11 and 16 GHz. The resonator is made of Copper with conductivity of $\sigma = 5.8 \cdot 10^7$ S/m. For this design the simulated unloaded Q-factor with HFSS eigenmode solver was found to be $Q_U = 4510$ at $f_o = 13.2954$ GHz.

Fig. 1(b) shows the 2D color plot of the absolute value of E-field from top view in the middle of the air gap. The third order mode is defined by the resonant length of the ridge. The quasi-TEM mode is resonating along the ridge, whereas the fields decay very fast sideways in all other directions due to cut-off provided by the pin surface.

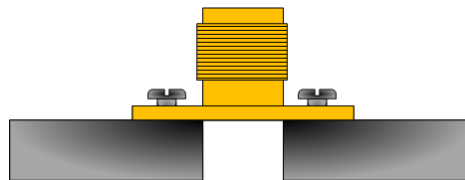
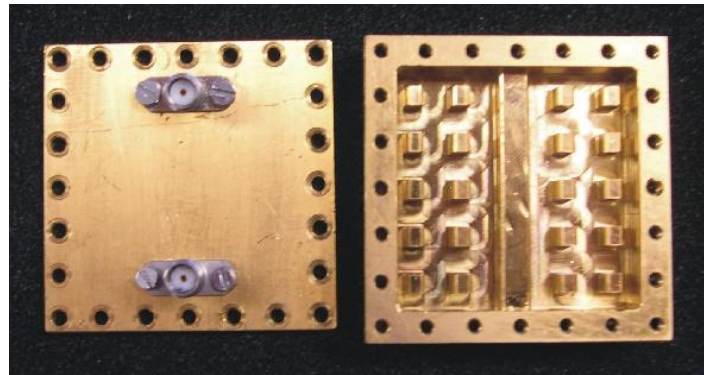
An experimental resonator was manufactured and measured using coaxial probes connected to a network analyzer. A photo of the prototype is shown in Fig. 1(c). The feeding is provided by SMA connectors on the upper plate, at the opposite ends of the ridge. Inner conductors of the SMAs are cut up to the upper side of the lid, as shown in the figure, in order to weakly couple to the resonator and thereby make the external Q-factor large. Fig. 1(d) shows simulated and measured results. Simulations are in this case carried out with HFSS, which has already been tested as an accurate electromagnetic simulation tool for resonant cavities [27]. The unloaded Q-factor can be calculated using (4) achieving $Q_U = 2255$ at $f_o = 13.3048$ GHz for the measured prototype and $Q_U = 4741$ at $f_o = 13.2757$ GHz for the simulated structure.



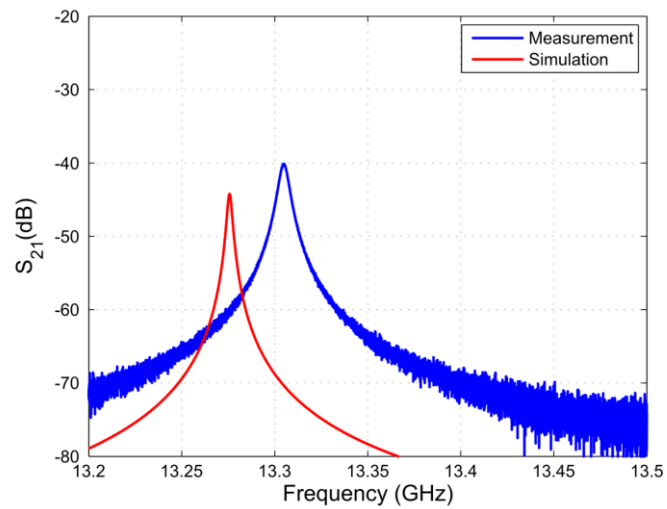
(a)



(b)



(c)



(d)

Fig. 1. (a) Geometry of short circuit ridge gap waveguide resonator. (b) 2D color plot of absolute value of E-field in the air gap between the ridge and the upper plate. (c) Resonator prototype and drawing of front view of SMA connector on top lid (inner conductor and dielectric of SMA are cut to obtain the weak coupling). (d) Measurement and simulation results for the short circuit ridge gap resonator.

The difference between measured and simulated Q s is mainly due to two factors: one is the surface roughness, and the other is the leakage from those sides of the box that are not surrounded by pins. The visually observable surface roughness is due to microscale irregularities in the surface, and it depends not only on the metal used (Copper in this case) but also on the fabrication technique (milling). When the skin depth is smaller than the height of the irregularities, the current will follow all the surface contours increasing its total path. This results in decreasing the conductivity of the material and increasing the conductor loss [28]. At 13 GHz the skin depth is 0.5 μm and for our case the metal used has an rms surface roughness varying between 1.5 and 3 μm . There could also be uncertainties due to the purity of the Copper material itself.

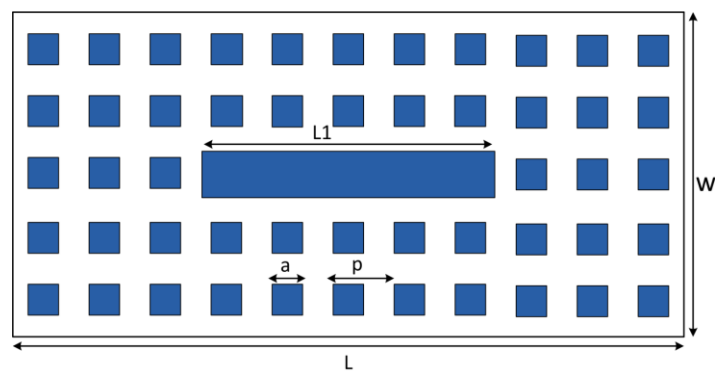
The leakage is a critical factor and it is the main cause of loss for waveguide components (when no substrate is used). In this design, the field is concentrated in a 3 mm air gap between the ridge and the lid. The leakage is prevented by the pins on the two sides of the ridge, whereas there are no pins at the two ends of it. The ends are directly short-circuited by a metal wall and the lid. There may be a small gap between the lid and the end walls, in particular if there are not enough screws fixing the lid to the end walls. Any leakage between the lid and end wall will reduce the Q . The difference in numerical and measured resonant frequencies is 0.21%, which is quite acceptable considering mechanical tolerances.

B. Open Circuit Resonator

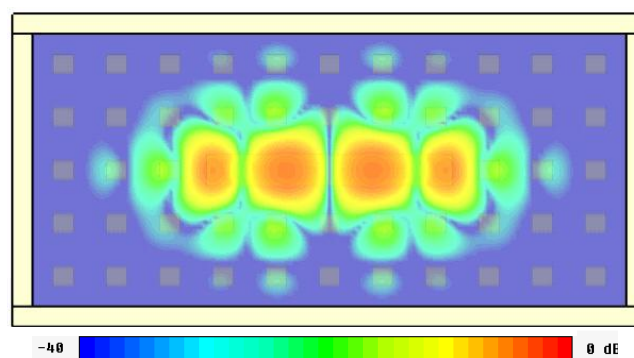
A second ridge gap waveguide resonator has been realized in order to remove the uncertainty in Q due to the leakage between the end walls and the lid, seen in the subsection above. The ridge gap waveguide geometry is similar to the previous one, but in this case we have an open circuit transmission line resonator obtained by adding three pin rows outside both ends of the ridge as shown in Fig. 2(a). For this geometry the dimensions are $L = 89$ mm, $W = 41$ mm, $p = 8$ mm, $L_1 = 37$ mm with reference to Fig. 2(a). The width a and length d of the pins, and the air gap h are the same as for the short-circuited resonator. The unloaded Q computed with HFSS eigenmode solver is $Q_U = 4437$ at $f_o = 13.2155$ GHz. 2D color plot of the absolute value of E-field is presented in Fig. 2(b), where the third order mode is shown for the open circuit transmission line resonator. The prototype has been manufactured and it is shown in Fig. 2(c). The excitation of the resonator is exactly as before. As shown in the color plot, the field is concentrated in the air gap between the ridge and the lid, and it is stopped by the pins in all other directions. Therefore, for this solution there is not leakage loss from imperfect metal contacts or tiny gaps between wall and lid. The simulated and measured transmission coefficients S_{21} are presented in Fig. 2(d). Again, by applying (4) we obtain $Q_U = 4130$ at $f_o = 13.1832$ GHz for the measured case, and $Q_U = 4603$ at $f_o = 13.1888$ GHz for the simulated case. Simulated and measured resonant frequencies agree very well with a deviation of 0.04 %. The difference between computed and measured Q -factors is 10.2% and it is believed to be mainly due to the surface roughness, which is not considered in simulations, as said before. The

losses of the gap waveguide can be directly calculated by applying (1). From our simulation, the losses are found to be 0.26 dB/m.

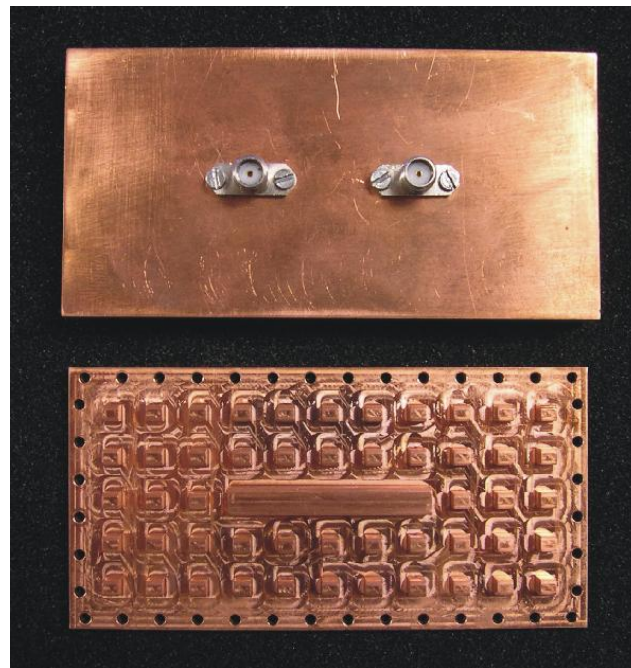
Comparisons between measured and simulated results for both short-circuit and open-circuit ridge gap waveguide resonators are summarized in Table I. The resonant frequency for the second design has moved down by a factor 0.121 compared to the short circuited design. The reason is that the reactive field at both resonator ends increases the effective resonance length, as shown in Fig. 2(b). The loss due to the leakage has been removed by the pins making the circuit less sensitive to manufacturing tolerances and increasing the measured Q of the open circuit resonator, which is 90% of the simulated value.



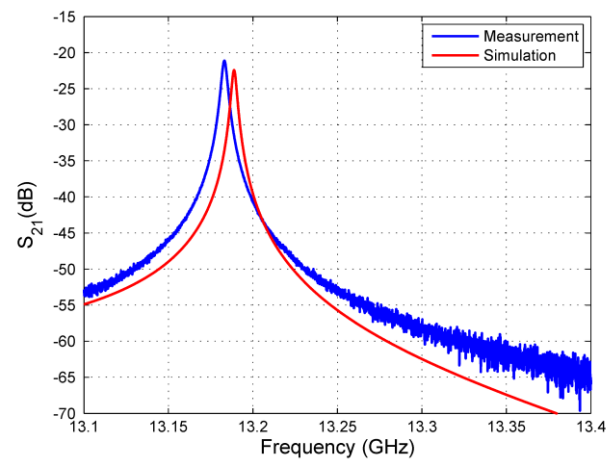
(a)



(b)



(c)



(d)

Fig. 2. (a) Geometry of open circuit ridge gap waveguide resonator (top view), with pins added before and after the ridge. (b) 2D color plot of absolute value of E-field. (c) Open circuit resonator prototype. (d) Simulation and measurement results for the open circuit ridge gap waveguide resonator.

IV. GROOVE GAP WAVEGUIDE RESONATOR

A short circuit resonator made in groove gap waveguide will be presented in this section. In this case, the ridge is removed and the field is propagating in the groove between the pins and the upper plate. This configuration behaves similarly as standard

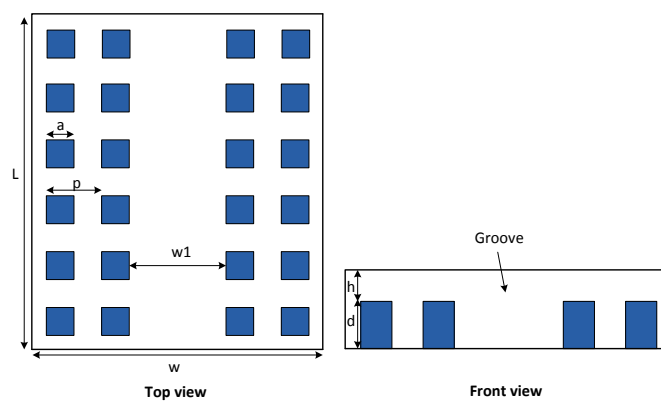
waveguides, with the difference that there is no need of contact between the bottom plate, with pins and groove, and the upper lid, as presented in [12].

A. Resonator Design

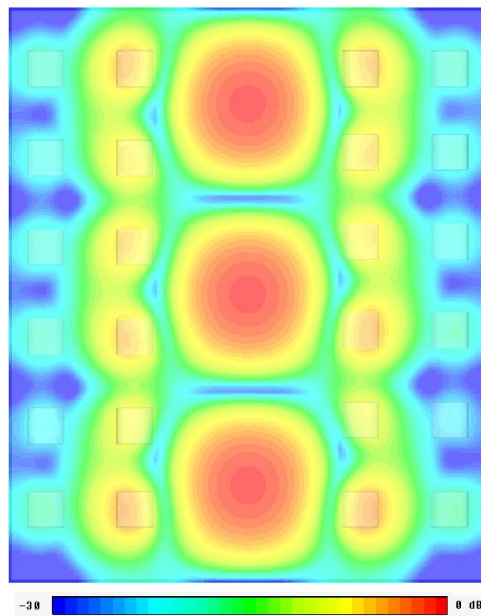
The geometry is presented in Fig. 3(a). The size of the box is 48×40 mm, period $p = 7.5$ mm, pins side $a = 3$ mm, pins length $d = 5$ mm and air gap $h = 3$ mm. For a fair comparison in terms of losses the dimensions of the cavity (groove) are the same as for the rectangular waveguide WR-62, working in the same frequency band, Ku band. Therefore, the groove width is $w_1 = 16$ mm and the total groove height is $(h + d) = 8$ mm. Also for this design the pins edges are rounded. The structure was first simulated with HFSS eigenmode solver and the unloaded Q for the third order mode was found to be $Q_U = 6534$ at $f_o = 13.5077$ GHz. 2D color plot of the absolute value of E-field is presented in Fig. 3(b), where the TE_{103} mode is propagating in the groove between the pins surface. The 2D plot cut is taken in the gap between the pins and the lid, i.e., at a distance $h/2$ from the lid, and this shows how the pins surface works ideally as a wall, since the field is attenuated by almost 30 dB after two pin rows.

B. Experimental Validation

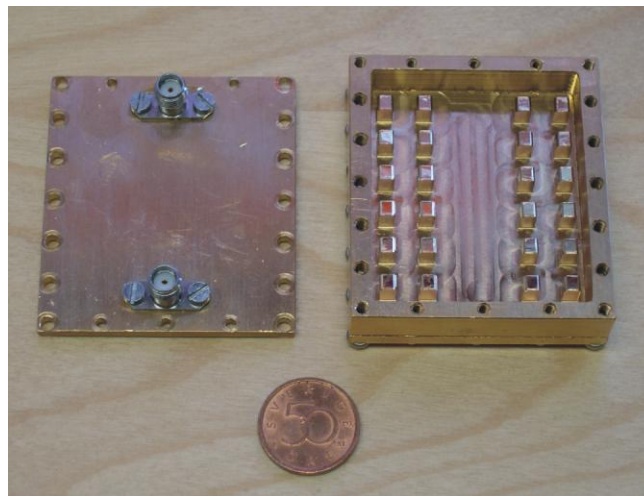
A resonator in groove gap waveguide was manufactured and measured in order to determine the Q-factor. The metal used was Copper. The prototype is presented in Fig. 3(c). The feeding is provided by SMA connectors from the top lid and the weak coupling is obtained by cutting their inner conductors, as already shown for the ridge case. Simulated and measured results are included in Fig. 3(d). Again, using equation (4) Q_U can be extracted from Q_L , obtaining $Q_U = 6136$ at $f_o = 13.4996$ GHz for the simulated structure whereas $Q_U = 5200$ at $f_o = 13.472$ GHz for the measurement.



(a)



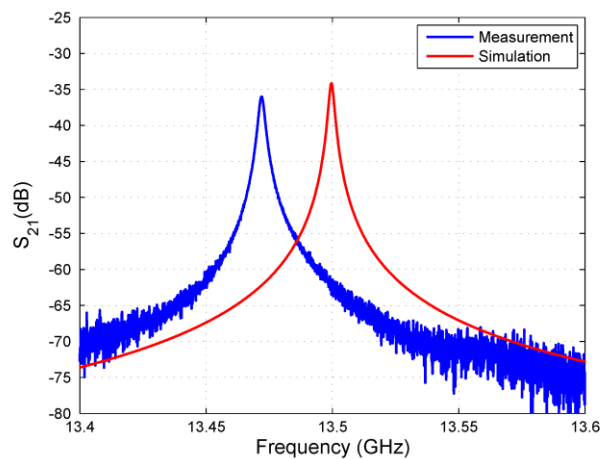
(b)



(c)

The discrepancy between simulation and measurement is due to the surface roughness and a residual leakage between the two end walls and the lid. Since any small gap can allow a certain amount of energy to leak from the resonator, another prototype was manufactured adding three rows of pins at both ends of the groove, in the same way as for the ridge gap resonator. A photo of this second circuit is shown in Fig. 4(a). Fig. 4(b) shows the 2D color plot of the E-field for the third mode at a distance $h/2$ from the top lid. As we can see from the color plot, the structure behaves as a short circuit resonator in contrast to the ridge gap waveguide with pin rows at both ends, which became an open circuit, as shown in Fig. 2(b). This is expected since between the ridge and the

first pin row there is a small space, whereas the groove is surrounded by pins behaving as metal walls. Consequently, the field will be short circuited at the pins boundary. The simulated and measured transmission coefficients for this resonator are presented in Fig. 4(c). The measured Q_U is 5883 at $f_o = 13.4434$ GHz and the computed Q_U is 6108 occurring at $f_o = 13.4617$ GHz, for the second resonator. The Q values for the first and the second (with more pins) groove gap resonators are also summarized in Table I. The measured Q is about 96% of the simulated one for the second groove gap resonator. The difference in resonant frequencies is 0.13% between simulation and measurement. Also in this case the resonant frequency has moved down for the second design compared to the first groove resonator, since the field is spreading over the first pins row when the pins are added at the ends of the groove, increasing the total resonant length. The pins at the end walls lead to an increase of the Q from 85% to 96% of its simulated value.

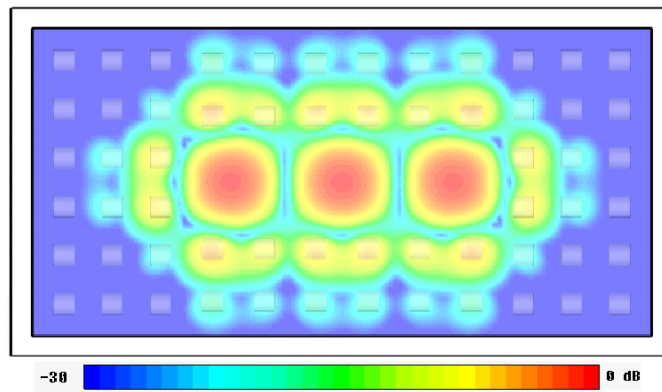


(d)

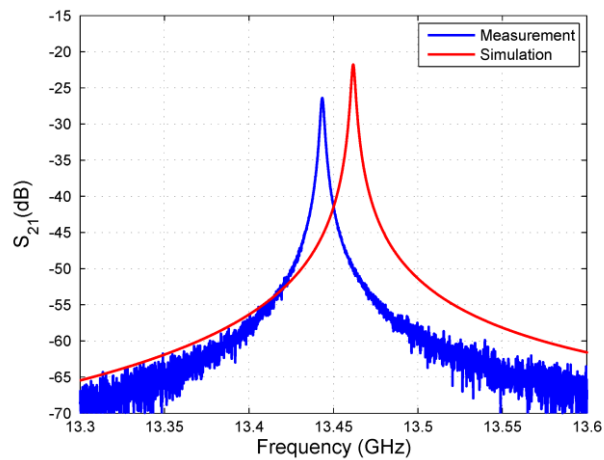
Fig. 3. (a) Groove gap waveguide resonator geometry. (b) 2D color plot of the TE_{103} . Plot cut is taken at a distance $h/2$ from the top lid. (c) Groove gap resonator prototype. (d) Simulated and measured transmission coefficients for the groove gap waveguide resonator.



(a)



(b)



(e)

Fig. 4. (a) Groove gap waveguide resonator prototype with three pin rows added before and after the groove. (b) 2D color plot of the TE_{103} for the groove gap resonator with more pins. Plot cut is taken at $h/2$, in the gap between the pins and the upper plate. (c) Simulated and measured transmission coefficients for the groove gap waveguide resonator with more pins.

V. COMPARISON BETWEEN STANDARD RECTANGULAR WAVEGUIDE AND GROOVE GAP WAVEGUIDE RESONATORS

It is well known that standard rectangular waveguides have low loss. In [23] it is shown that ideal rectangular waveguides can have very high Q_U , in the order of 8000 at 13.5 GHz. However, in reality these structures are affected by many factors during the fabrication process, which contribute to lower the Q-factor. In particular, not perfect alignment between the metal blocks can cause leakage of energy from the cavity. Also, many screws are needed in order to assure good contacts and avoid radiation loss. Indeed, in [29] it is stated that typically it is only possible to realize 65-80 % of the theoretical Q factor of standard waveguides. This problem becomes more critical while working at high frequency as the circuitry becomes smaller and very sensitive to any small variation, rising manufacturing costs and production complexity. On the other hand, the gap waveguide technology allows TEM or TE/TM modes without a need of contact between the upper and lower plates obtained by using pins walls instead of smooth metal walls. To better understand this concept, a rectangular waveguide resonator, working between 12 and 18 GHz, has been manufactured, measured and compared with the first groove gap resonator presented in Section IV. The waveguide is realized by joining the upper plate to the bottom box with screws and has the same width and height as for the groove gap waveguide resonator, i.e., 16 mm and 8 mm, respectively. The metal used is the same, i.e., Copper. Measurements are performed for three different cases for both resonators. Results are presented in Fig. 5 for the standard waveguide (Fig. 5(a)) and for the groove gap waveguide (Fig. 5(b)): in the first case (blue curves) the resonators are measured in a typical situation where the lid is

screwed to the box walls all the way around the rim. The measured Q_U is 5400 for the standard waveguide and 5200 for the groove gap waveguide. Thus, the Q of the groove gap waveguide is 96% of the Q of the standard rectangular waveguide.

In the second measurement set up, the groove gap resonator is measured when the screws along the sidewalls have been removed, i.e. there are screws along the end walls only. The same is done for the rectangular waveguide. As expected this causes leakage of energy from the joint between the sidewalls and the lid of the standard waveguide decreasing the Q -factor to 3079 (red curve). For the groove gap resonator, however, the Q does not change at all, showing that two pin rows are already enough to remove any losses due to electrical contact-problems between the sidewalls and the lid. In the third measurement, both resonators are measured with no screws in the lid, i.e. the lid is simply resting on the surrounding walls. In this case, both Q values decrease as expected and a lot of energy is leaking from the joint between the lid and the walls at those sides and ends where there are no pins. This means that the presence of pins is essential to provide high Q replacing the requirement for conductive contact across metal joints.

VI. CONCLUSION

The gap waveguide is a new technology, which can be used in many applications at low and high frequency. In this paper we focused on the study of losses of ridge and groove gap waveguides realized with metal pins. The study was based on theoretical and experimental determination of Q -factors of resonators working at around 13.3 GHz. All measured and simulated results are summarized in Table I. The first ridge gap waveguide resonator was realized by ending the metal ridge directly on a vertical metal wall in order to create a short circuit resonator. Simulation and measurement results showed a discrepancy in Q values. Therefore, a second ridge gap waveguide resonator was realized adding three rows of pins at both ends of the ridge. The new measured Q was 90% of the simulated one; the small difference is probably due to the surface roughness which was not considered in simulations. Therefore, we can conclude that the lower Q of the first short circuit resonator was due to the leakage between the vertical end walls and the lid.

It was shown that the ridge gap waveguide can provide Q -factors of around 4100 and even higher if silver plating is provided. From the measured results the corresponding attenuation in the open circuit ridge gap resonator was found to be 0.29 dB/m, much lower than microstrip transmission lines, having typical loss of 3-4 dB/m (at the same frequency) when using a low loss dielectric substrate, e.g., Duroid 5880 ($\epsilon_r = 2.2$ and $\tan\delta = 0.0009$). We also studied a groove gap waveguide, which works similarly as standard rectangular waveguides. The measured Q -factor was found to be 5200 when there were no pins at the ends of the resonator, and 5883 when we added pin rows around the whole resonant groove.

Groove gap waveguide has higher Q factor than the ridge gap. The Q increases with the vertical height of the waveguide and for the groove case the total height is $(h + d) = 8$ mm, whereas for the ridge gap the field is propagating along the air gap of height h

= 3 mm. The problem with leakage at end walls is larger with ridge because then the joint towards the lid becomes larger compared to the total height of the wall than in a groove gap waveguide case.

In Section V it was shown that groove gap and rectangular waveguides have similar measured Q values. It is indeed true that rectangular waveguides can reach ideally larger Q s, but as already said, mechanical issues affect their performance. In this case the measured Q factor of the standard waveguide is about 64% of the theoretical value, while the measured Q of the groove gap waveguide approaches the theoretical one by 96 %. On the other hand, the simulated and measured resonant frequencies differ more for the groove gap waveguide compared to the rectangular waveguide. However, still this variation is low, as can be seen from Table I. The 0.135% difference in resonant frequencies for the groove case can be due to tolerances in the manufactured prototype. The resonant length of the groove prototype can be affected by tolerances on the position of the pin walls, compared to the rectangular waveguide which has smooth metal walls.

TABLE I

COMPARISONS OF SIMULATED AND MEASURED RESULTS FOR RIDGE GAP WAVEGUIDES, GROOVE GAP WAVEGUIDES AND
RECTANGULAR WAVEGUIDE

	Simulations				Measurements			Differences (%)		
	Q (Eigenmode)	Q (S_{21})	f (GHz)	α (dB/m)	Q (S_{21})	f (GHz)	α (dB/m)	Q (S_{21})	f	α
Short Circuit Ridge Gap Resonator	4510	4741	13.2757	0.254	2255	13.3048	0.535	52.4	0.21	52.2
Open Circuit Ridge Gap Resonator	4437	4603	13.1888	0.26	4130	13.1832	0.29	10.2	0.04	10.3
First Groove Gap Resonator	6534	6136	13.4996	Not TEM line	5200	13.472	Not TEM line	15.25	0.2	Not TEM line
Second Groove Gap Resonator (with more pins)	6265	6108	13.4617	Not TEM line	5883	13.4434	Not TEM line	3.68	0.135	Not TEM line
Rectangular Waveguide WR-62	8499	8464	13.5434	Not TEM line	5400	13.5444	Not TEM line	36.20	0.007	Not TEM line

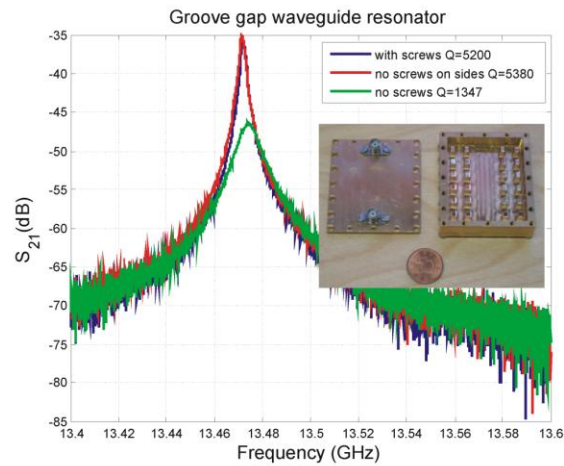
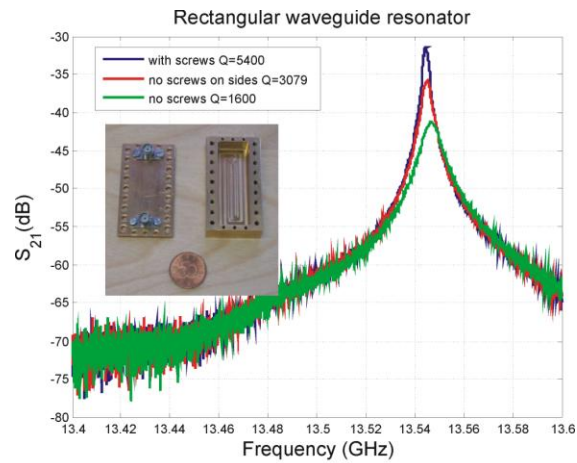


Fig. 5. Measured transmission coefficients for rectangular waveguide (a) and groove gap waveguide (b) resonators. Measurements are done for three different cases. In the first (blue curves), the circuits are measured when the top lid is connected to the bottom one with screws in all sides. In the second case (red curves), screws are removed on sides walls. In the third (green curves), the resonators are measured without any screw between lid and circuit for both resonators.

ACKNOWLEDGMENT

This work has been supported mainly by the Swedish Research Council VR and partly by Swedish Strategic Research Foundation (SSF) within the Chalmers Microwave Antenna Systems Research Center (CHARMANT).

REFERENCES

- [1] P.-S. Kildal, E. Alfonso, A. Valero-Nogueira, E. Rajo-Iglesias, "Local metamaterial-based waveguides in gaps between parallel metal plates", *IEEE Antennas and Wireless Propagation Letters*, Vol. 8, pp. 84-87, 2009.
- [2] P.-S. Kildal, "Three metamaterial-based gap waveguides between parallel metal plates for mm/submm waves", *European Conference on Antennas and Propagation (EuCAP 2009)*, Berlin, Germany, 2009.
- [3] E. Alfonso, P. Kildal, A. Valero, J. I. Herranz, "Numerical analysis of a metamaterial-based ridge gap waveguide with a bed of nails as parallel-plate mode killer", *European Conference on Antennas and Propagation (EuCAP 2009)*, Berlin, Germany, 2009.
- [4] M. G. Silveirinha, C. A. Fernandes, and J. R. Costa, "Electromagnetic characterization of textured surfaces formed by metallic pins," *IEEE Transactions on Antennas and Propagation*, vol. 56, no. 2, pp. 405–415, 2008.
- [5] D. Sievenpiper, Z. Lijun, R. F. J. Broas, N. G. Alexopolous, and E. Yablonovitch, "High-impedance electromagnetic surfaces with a forbidden frequency band", *IEEE Transactions on Microwave Theory and Techniques*, vol. 47, no. 11, pp. 2059–2074, 1999.
- [6] E. Rajo-Iglesias and P. S. Kildal, "Numerical studies of bandwidth of parallel-plate cut-off realized by a bed of nails, corrugations and mushroom-type electromagnetic bandgap for use in gap waveguides", *IET Microwaves, Antennas & Propagation*, vol. 5, pp. 282-289, 2011.
- [7] P. S. Kildal, A. U. Zaman, E. Rajo-Iglesias, E. Alfonso, and A. Valero-Nogueira, "Design and experimental verification of ridge gap waveguide in bed of nails for parallel-plate mode suppression", *IET Microwaves, Antennas & Propagation*, vol. 5, no. 3, pp. 262–270, 2011.
- [8] P.-S. Kildal, "Artificially soft and hard surfaces in electromagnetics", *IEEE Transaction on Antennas and Propagation*, vol. 28, no. 10, pp. 1537–1544, 1990.
- [9] M. N. M. Kehn and P. S. Kildal, "Miniaturized rectangular hard waveguides for use in multifrequency phased arrays", *IEEE Transactions on Antennas and Propagation*, vol. 53, no. 1, pp. 100–109, 2005.
- [10] P.-S. Kildal and M. N. M. Kehn, "The ridge gap waveguide as a wideband rectangular hard waveguide", *Fourth European Conference on Antennas and Propagation (EuCAP 2010)*, pp. 1–4.
- [11] A. Valero-Nogueira, E. Alfonso, J. I. Herranz, P.-S. Kildal, "Experimental demonstration of local quasi-TEM gap modes in single-hard-wall waveguides", *IEEE Microwave and Wireless Components Letters*, Vol. 19, No. 9, pp. 536-538, Sept. 2009.
- [12] E. Rajo-Iglesias and P.-S. Kildal, "Groove gap waveguide: a rectangular waveguide between contactless metal plates enabled by parallel-plate cut-off", *Fourth European Conference on Antennas and Propagation (EuCAP 2010)*, pp. 1–4.
- [13] H. Uchimura, T. Takenoshita, and M. Fujii, "Development of "laminated waveguide", *IEEE Transactions on Microwave Theory and Techniques*, vol. 46, no. 12, pp. 2438–2443, 1998.
- [14] J. Hirokawa and M. Ando, "Single-layer feed waveguide consisting of posts for plane TEM wave excitation in parallel plates," *IEEE Trans. Antennas Propag.*, vol. 46, no. 5, pp. 625–630, May 1998.
- [15] D. Stephens, P. R. Young, and I. D. Robertson, "Millimeter-wave substrate integrated waveguides and filters in photoimageable thick-film technology", *IEEE Transactions on Microwave Theory and Techniques*, Vol. 53, No. 12, pp. 3832-3838, December 2005.
- [16] E. Rajo-Iglesias, A. U. Zaman, and P. S. Kildal, "Parallel plate cavity mode suppression in microstrip circuit packages using a lid of nails", *IEEE Microwave and Wireless Components Letters*, vol. 20, no. 1, pp. 31–33, 2010.
- [17] A. Polemi, S. Maci, P.-S. Kildal, "Dispersion characteristics of metamaterial-based parallel-plate ridge gap waveguide realized by bed of nails", *IEEE Transactions on Antennas and Propagation*, Vol. 59, No. 3, pp. 904-913, March 2011.

- [18] M. Bosiljevac, Z. Sipus, P.-S. Kildal, "Construction of Green's functions of parallel plates with periodic texture with application to gap waveguides - A plane wave spectral domain approach", *IET Microwave, Antennas & Propagation*, Vol. 4, no. 11, pp. 1799–1810, Nov. 2010.
- [19] H. Raza, J. Yang, T. Östling, "A low loss rat race balun in gap waveguide technology", *European Conference on Antennas and Propagation (EuCAP 2011)*, Rome, April 11-16.
- [20] E. Alfonso Alós, A. U. Zaman, and P.-S. Kildal, "Ka-Band Gap Waveguide Coupled-Resonator Filter for Radio Link Diplexer Application", *IEEE Transactions on Components, Packaging and Manufacturing Technology*, vol. PP, no. 99, 2013.
- [21] A. U. Zaman, P.-S. Kildal, and A. A. Kishk, "Narrow-Band Microwave Filter Using High-Q Groove Gap Waveguide Resonators with Manufacturing Flexibility and No Sidewalls," *IEEE Transactions on Components, Packaging and Manufacturing Technology*, vol.2, no.11, pp.1882-1889, Nov. 2012.
- [22] H. Kirino, K. Ogawa, "A 76 GHz Multi-Layered Phased Array Antenna Using a Non-Metal Contact Metamaterial Waveguide," *IEEE Transactions on Antennas and Propagation*, vol.60, no.2, pp.840,853, Feb. 2012.
- [23] E. Pucci, A. U. Zaman, E. Rajo-Iglesias, P.-S. Kildal, and A. Kishk, "Losses in ridge gap waveguide compared with rectangular waveguides and microstrip transmission lines," *Fourth European Conference on Antennas and Propagation (EuCAP 2010)*, pp. 1–4.
- [24] D. M. Pozar, *Microwave Engineering*, Sec. 6, 3rd ed. Wiley.
- [25] J. Papapolymerou, C. Jui-Ching, J. East, and L. P. B. Katehi, "A micromachined high-Q X-band resonator", *IEEE Microwave and Guided Wave Letters*, vol. 7, no. 6, pp. 168–170, 1997.
- [26] D. Kajfez, "*Q Factor*", Vector Fields, Oxford, MS, 1994.
- [27] T. H. Tran, Y. F. She, J. Hirokawa, K. Sakurai, Y. Kogami, and M. Ando, "Evaluation of effective conductivity of copper-clad dielectric laminate substrates in millimeter-wave bands using whispering gallery mode resonators", *IEEE Transactions on Electronics*, vol. E92C, no. 12, pp.1504–1511, 2009.
- [28] M. Koledintseva, A. Koul, F. Zhou, J. Drewniak, and S. Hinaga, "Surface impedance approach to calculate loss in rough conductor coated with dielectric layer", *IEEE International Symposium on Electromagnetic Compatibility (EMC), 2010* .
- [29] C. Kudsia, R. Cameron, and W.-C. Tang, "Innovations in microwave filters and multiplexing networks for communications satellite systems", *IEEE Transaction on Microwave Theory and Techniques*, Vol. 40, No. 6, pp.1133–1149, June 1992.